Acta Cryst E CRYSTALLOGRAPHIC COMMUNICATIONS
ISSN 2056-9890

Crystal structure, Hirshfeld surface analysis and DFT studies of 6-[(*E*)-2-(thiophen-2-yl)ethenyl]-4,5-dihydropyridazin-3(2*H*)-one

Said Daoui,[a] Emine Berrin Çınar,[b]* Fouad El Kalai,[a]* Rafik Saddik,[c] Necmi Dege,[b]* Khalid Karrouchi[d] and Noureddine Benchat[a]

[a]Laboratory of Applied Chemistry and Environment (LCAE), Faculty of Sciences, Mohamed I University, 60000 Oujda, Morocco, [b]Department of Physics, Faculty of Arts and Sciences, Ondokuz Mayıs, University, Samsun, Turkey, [c]Laboratory of Organic Synthesis, Extraction and Valorization, Faculty of Sciences, Ain Chok, University Hassan II, Casablanca, Rabat, Morocco, and [d]Laboratory of Plant Chemistry, Organic and Bioorganic Synthesis, URAC23, Faculty of Science, BP 1014, GEOPAC Research Center, Mohammed V University, Rabat, Morocco. *Correspondence e-mail: emineberrin.cinar@omu.edu.tr, fouadelkalai80@gmail.com, necmid@omu.edu.tr

Received 17 September 2019
Accepted 9 November 2019

Edited by J. T. Mague, Tulane University, USA

Keywords: crystal structure; dihydropyridazine; DFT; molecular electrostatic potential; pyridazine; thiophen.

CCDC reference: 1964913

Supporting information: this article has supporting information at journals.iucr.org/e

In the title compound, $C_{10}H_{10}N_2OS$, the five atoms of the thiophene ring are essentially coplanar (r.m.s. deviation = 0.0037 Å) and the pyridazine ring is non-planar. In the crystal, pairs of N—H···O hydrogen bonds link the molecules into dimers with an $R_2^2(8)$ ring motif. The dimers are linked by C—H···O interactions, forming layers parallel to the *bc* plane. The theoretical geometric parameters are in good agreement with XRD results. The intermolecular interactions were investigated using a Hirshfeld surface analysis and two-dimensional fingerprint plots. The Hirshfeld surface analysis of the title compound suggests that the most significant contributions to the crystal packing are by H···H (39.7%), C···H/H···C (17.3%) and O···H/H···O (16.8%) contacts.

1. Chemical context

Pyridazinone derivatives have been tested for their chemical and biological properties and achieved an increased interest in recent years (Akhtar *et al.*, 2016). The pyridazinone moiety is known as a 'wonder nucleus' as it can form diverse derivatives with many types of pharmacological activities such as anti-depressant (Boukharsa *et al.*, 2016), anti-HIV (Livermore *et al.*, 1993), anti-inflammatory (Barberot *et al.*, 2018), anti-convulsant (Partap *et al.*, 2018), antihistaminic (Tao *et al.* 2012) and glucan synthase inhibition (Zhou *et al.*, 2011) as well as acting as herbicidal agents (Asif, 2013). We report the synthesis and the crystal and molecular structure of the title compound (Fig. 1), as well as an analysis of its Hirshfeld surface and DFT studies.

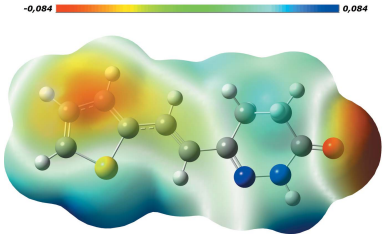

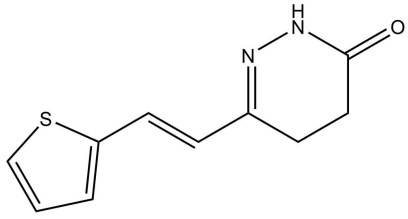

2. Structural commentary

Selected geometrical parameters are given in Table 1. The five atoms of the thiophene ring are essentially coplanar (r.m.s.

Table 1
Selected bond lengths, angles and torsion angles (Å, °).

	X-ray	DFT/B3LYP/LANL2DZ
S1—C10	1.691 (3)	1.734 (7)
O1—C1	1.227 (3)	1.219 (9)
N2—C4	1.283 (3)	1.300 (2)
N2—N1	1.385 (2)	1.375 (6)
N1—C1	1.345 (3)	1.353 (0)
C10—S1—C7	92.31 (13)	91.705 (6)
O1—C1—N1	121.4 (2)	121.412 (2)
C7—C6—C5—C4	179.0 (2)	178.857 (8)
N2—C4—C5—C6	−179.4 (2)	179.554 (8)

deviation = 0.0037 Å) while the pyridazine ring is non-planar with atom C2 furthest from the mean molecular plane at a distance of 0.610 (5) Å.

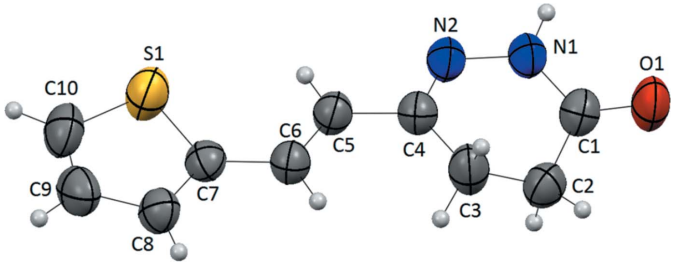

Figure 1
Molecular structure of the title compound showing the atom labelling and displacement ellipsoids drawn at the 50% probability level.

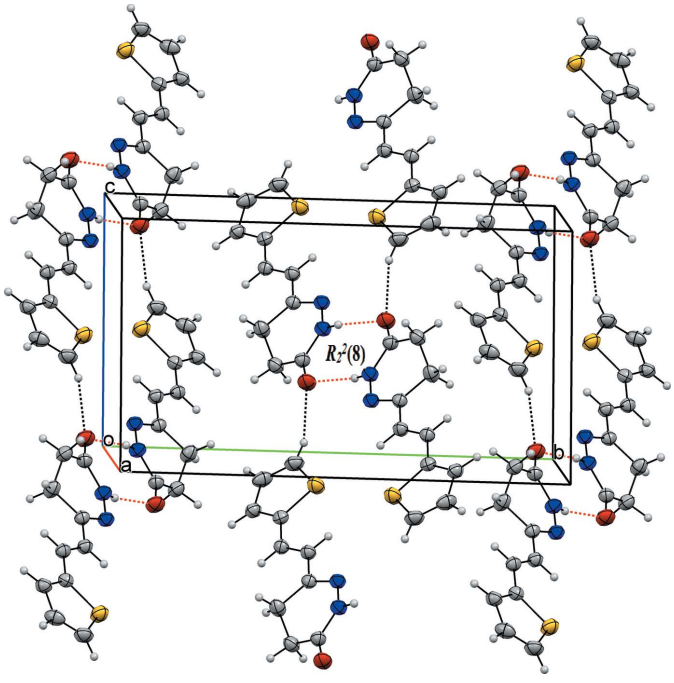

Figure 2
Inversion dimers with $R_2^2(8)$ ring motifs formed by N—H···O hydrogen bonds (red dashed lines; Table 2). C—H···O interactions are shown as black dashed lines.

Table 2
Hydrogen-bond geometry (Å, °).

D—H···A	D—H	H···A	D···A	D—H···A
N1—H1···O1^{i}	0.83 (3)	2.07 (3)	2.899 (3)	175 (2)
C10—H10···O1^{ii}	0.93	2.61	3.505 (3)	161

Symmetry codes: (i) $-x+2, -y+1, -z+1$; (ii) $x-1, y, z+1$.

3. Supramolecular features

In the crystal, the molecules are connected pairwise through N—H···O hydrogen bonds (Table 2), forming dimers with an $R_2^2(8)$ graph set motif. The dimers are linked by C—H···O hydrogen bonds, forming layers parallel to the *bc* plane (Fig. 2). A packing diagram is shown in Fig. 2.

4. Database survey

A search of the Cambridge Structural Database (CSD, version 5.40, update November 2018; Groom *et al.*, 2016) using (*E*)-6-(thiophen-2-yl)hex-5-enal and 6-vinyl-4,5-dihydropyridazin-3(2*H*)-one as the main skeleton found two structures similar to the title compound containing the pyridazine moiety with different substituents: 4-chloro-2-[(5-ethoxy-1,3,4-thiadiazol-2-yl)methyl]-5-(piperidin-1-yl)pyridazin-3(2*H*)-one (DOPZAL; Li *et al.*, 2014) and 4-[(*tert*-butyldiphenylsilyloxy)methyl]pyridazin-3(2*H*)-one (CISPAX; Costas-Lago *et al.*, 2013). In DOPZAL, the six atoms of the 1,6-dihydropyridazine ring are essentially coplanar (r.m.s. deviation = 0.008 Å), and the dihedral angle between this and the 1,3,4-thiadiazole ring is 62.06 (10)°. In CISPAX, pyridazinone moieties are anti-oriented across the Si—O bond [torsion angle = 168.44 (19)°]. In the crystal, molecules are assembled into inversion dimers through co-operative N—H···O hydrogen bonds between the NH groups and O atoms of the pyridazinone rings of neighbouring molecules.

5. Surface Analysis (SA)

The Hirshfeld surface analysis (Spackman & Jayatilaka, 2009) and the associated fingerprint plots were performed with *CrystalExplorer17.5* (Turner *et al.*, 2017). This software was used to analyse the intermolecular interactions in the crystal and to generate fingerprint plots mapped over d_{norm}, shape index and curvedness (Fig. 3). The Hirshfeld surface was calculated using a standard (high) surface resolution with the three-dimensional d_{norm} surface plotted over a fixed colour

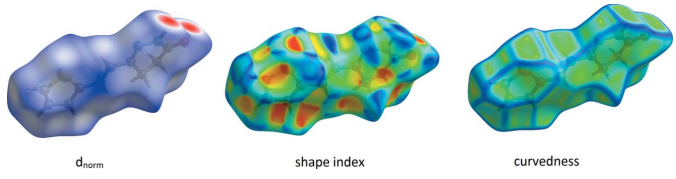

Figure 3
The Hirshfeld surfaces of the title compound mapped over d_{norm}, shape-index and curvedness.

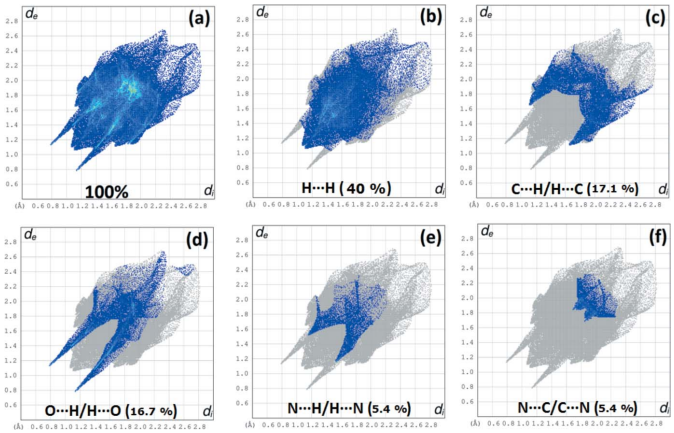

Figure 4
Two-dimensional fingerprint plots for the title compound, with a d_{norm} view and the relative contributions of the atom pairs to the Hirshfeld surface.

scale of −0.532 (red) to 1.345 (blue) a.u. The pale-red spots symbolize short contacts and negative d_{norm} values on the surface correspond to the N—H···O and C—H···O interactions (Table 2). The overall fingerprint plot and those delineated into H···H, H···C/ C···H, H···O/O···H, N···H/H···N and N···C/C···N contacts are shown in Fig. 4 along with their relative contributions to the Hirshfeld surface. The largest contribution is from H···H interactions (40.0%). The shape-index map of the title complex was generated in the range −1 to 1 Å, with the convex blue regions indicating hydrogen-donor groups and the concave red regions hydrogen-acceptor groups. The curvedness map, generated in the range −4 to 0.4 Å, shows large regions of green which denote a relatively flat surface area (planar), while the blue regions denote areas of curvature.

A view of the molecular electrostatic potential, in the range − 0.084 to 0.084 a.u. generated by the DFT method using the 6-31G(d,p) basis set is shown in Fig. 5. Here the N—H···O hydrogen-bond donors and acceptors are shown as blue and red areas around the atoms related with positive (hydrogen-bond donors) and negative (hydrogen-bond acceptors) electrostatic potentials, respectively.

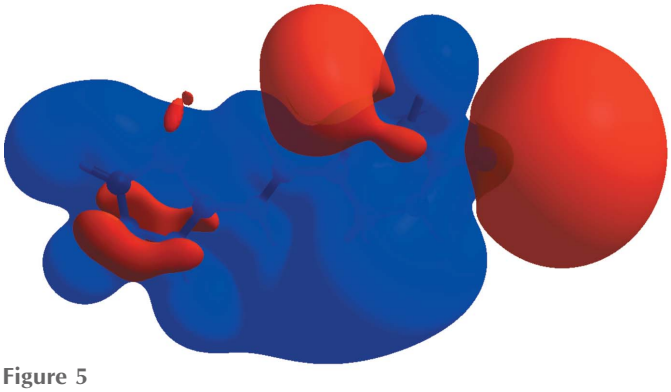

Figure 5
A view of the molecular electrostatic potential for the title compound in the range −0.084 to 0.084 a.u. generated by DFT using the 6–31G(d,p) basis set.

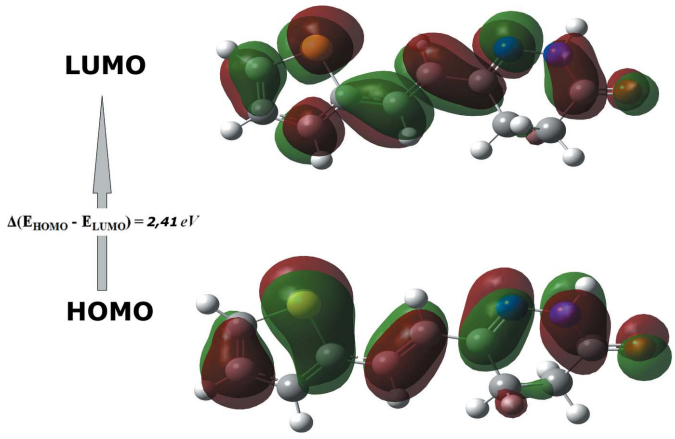

Figure 6
The electron distribution of the HOMO and LUMO energy gaps of the title compound.

The theoretical calculations were performed using *GAUSSIAN03* (Frisch *et al.*, 2004). The initial geometry was taken from the X-ray coordinates and this geometry was optimized using the DFT/B3LYP (Becke, 1993) method with LANL2DZ as the basis set. The theoretical geometrical parameters are in good agreement with XRD results (Table 1).

6. Frontier molecular orbitals

The highest occupied molecular orbitals (HOMO) and the lowest unoccupied molecular orbitals (LUMO) are known as frontier molecular orbitals (FMOs). The FMOs play an important role in the optical and electric properties. The frontier orbital gap can indicate the chemical reactivity and the kinetic stability of the molecule. If the energy gap is small then the molecule is highly polarizable and has high chemical reactivity. A molecule with a small frontier orbital gap is generally associated with a high chemical reactivity, low kinetic stability and is termed a soft molecule. Fig. 6 illustrates the HOMO and LUMO energy levels of the title compound. The small HOMO–LUMO energy gap of 2.41 eV in this

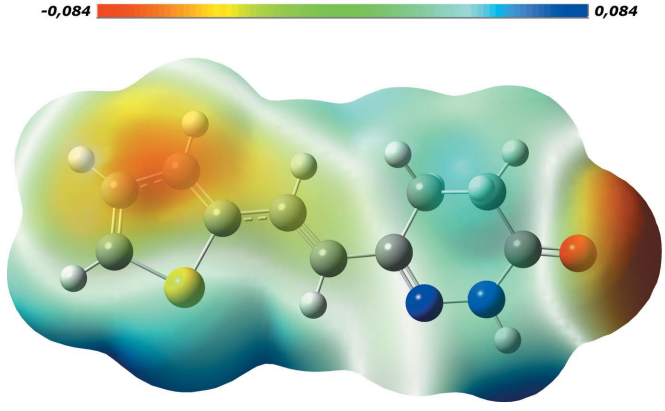

Figure 7
The total electron density three-dimensional surface mapped for the compound with the electrostatic potential calculated at the B3LYP/6–31G(d,p) level.

compound indicates the chemical reactivity is strong and the kinetic stability is weak. A map of the electron density is shown in Fig. 7.

7. Synthesis and crystallization

To a solution of 4-oxo-6-(thiophen-2-yl)hex-5-enoic acid (0.21 g, 1 mmol) in 20 mL of ethanol, it was added an equimolar amount of hydrazine hydrate. The mixture was maintained under reflux for 4h, until TLC indicated the end of the reaction. The reaction mixture was poured into cold water, and the precipitate formed was filtered out, washed with ethanol and recrystallized from ethanol. Slow evaporation at room temperature led to formation of single crystals.

8. Refinement

Crystal data, data collection and structure refinement details are summarized in Table 3. Hydrogen atoms were fixed geometrically and treated as riding, the C-bound H atoms were placed in idealized positions and refined as riding: C—H = 0.93 Å for methylene U_{iso}(H) = 1.5U_{eq}(C) and C—H = 0.97 Å for the other C atoms with U_{iso}(H) = 1.2U_{eq}(C). The NH H atom was located in a difference-Fourier map and freely refined.

Table 3
Experimental details.

Crystal data	
Chemical formula	$C_{10}H_{10}N_2OS$
M_r	206.26
Crystal system, space group	Monoclinic, $P2_1/c$
Temperature (K)	296
a, b, c (Å)	6.9932 (5), 16.2916 (9), 9.3544 (7)
β (°)	110.168 (6)
V (Å^3)	1000.40 (12)
Z	4
Radiation type	Mo $K\alpha$
μ (mm^{-1})	0.29
Crystal size (mm)	0.78 × 0.43 × 0.25
Data collection	
Diffractometer	Stoe *IPDS* 2
Absorption correction	Integration (*X-RED32*; Stoe & Cie, 2002)
T_{min}, T_{max}	0.767, 0.932
No. of measured, independent and observed [$I > 2\sigma(I)$] reflections	6292, 1971, 1394
R_{int}	0.043
(sin $\theta/\lambda)_{max}$ (Å^{-1})	0.617
Refinement	
$R[F^2 > 2\sigma(F^2)]$, $wR(F^2)$, S	0.045, 0.135, 1.02
No. of reflections	1971
No. of parameters	131
No. of restraints	19
H-atom treatment	H atoms treated by a mixture of independent and constrained refinement
$\Delta\rho_{max}$, $\Delta\rho_{min}$ (e Å^{-3})	0.24, −0.34

Computer programs: *X-AREA* and *X-RED32* (Stoe & Cie, 2002), *SHELXT2015* (Sheldrick, 2015*a*), *SHELXL2015* (Sheldrick, 2015*b*), *Mercury* (Macrae *et al.*, 2008), *WinGX* (Farrugia, 2012) and *PLATON* (Spek, 2009).

Funding information

This study was supported by Ondokuz Mayıs University under project No. PYO·FEN1906.19.001.

References

Akhtar, W., Shaquiquzzaman, M., Akhter, M., Verma, G., Khan, M. F. & Alam, M. M. (2016). *Eur. J. Med. Chem.* **123**, 256–281.

Asif, M. (2013). *Mini-Rev. Org. Chem.* **10**, 113–122.

Barberot, C., Moniot, A., Allart-Simon, I., Malleret, L., Yegorova, T., Laronze-Cochard, M., Bentaher, A., Médebielle, M., Bouillon, J., Hénon, E., Sapi, J., Velard, F. & Gérard, S. (2018). *Eur. J. Med. Chem.* **146**, 139–146.

Becke, A. D. (1993). *J. Chem. Phys.* **98**, 5648–5652.

Boukharsa, Y., Meddah, B., Tiendrebeogo, R. Y., Ibrahimi, A., Taoufik, J., Cherrah, Y., Benomar, A., Faouzi, M. E. A. & Ansar, M. (2016). *Med. Chem. Res.* **25**, 494–500.

Costas-Lago, M. C., Costas, T., Vila, N. & Besada, P. (2013). *Acta Cryst.* E**69**, o1859–o1860.

Farrugia, L. J. (2012). *J. Appl. Cryst.* **45**, 849–854.

Frisch, M. J., Trucks, G. W., Schlegel, H. B., Scuseria, G. E., Robb, M. A., Cheeseman, J. R., Montgomery, J. A. Jr, Vreven, T., Kudin, K. N., Burant, J. C., Millam, J. M., Iyengar, S. S., Tomasi, J., Barone, V., Mennucci, B., Cossi, M., Scalmani, G., Rega, N., Petersson, G. A., Nakatsuji, H., Hada, M., Ehara, M., Toyota, K., Fukuda, R., Hasegawa, J., Ishida, M., Nakajima, T., Honda, Y., Kitao, O., Nakai, H., Klene, M., Li, X., Knox, J. E., Hratchian, H. P., Cross, J. B., Bakken, V., Adamo, C., Jaramillo, J., Gomperts, R., Stratmann, R. E., Yazyev, O., Austin, A. J., Cammi, R., Pomelli, C., Ochterski, J. W., Ayala, P. Y., Morokuma, K., Voth, G. A., Salvador, P., Dannenberg, J. J., Zakrzewski, V. G., Dapprich, S., Daniels, A. D., Strain, M. C., Farkas, O., Malick, D. K., Rabuck, A. D., Raghavachari, K., Foresman, J. B., Ortiz, J. V., Cui, Q., Baboul, A. G., Clifford, S., Cioslowski, J., Stefanov, B. B., Liu, G., Liashenko, A., Piskorz, P., Komaromi, I., Martin, R. L., Fox, D. J., Keith, T., Al-Laham, M. A., Peng, C. Y., Nanayakkara, A., Challacombe, M., Gill, P. M. W., Johnson, B., Chen, W., Wong, M. W., Gonzalez, C. & Pople, J. A. (2004). *GAUSSIAN03*. Gaussian Inc., Wallingford, CT, USA.

Groom, C. R., Bruno, I. J., Lightfoot, M. P. & Ward, S. C. (2016). *Acta Cryst.* B**72**, 171–179.

Li, H., Ren, X., Li, Y. & Zhao, L. (2014). *Acta Cryst.* E**70**, o1113.

Livermore, D., Bethell, R. C., Cammack, N., Hancock, A. P., Hann, M. M., Green, D., Lamont, R. B., Noble, S. A., Orr, D. C., Payne, J. P., Ramsay, M. V. J., Shingler, A. H. Smith, C., Storer, R., Williamson, C. & Willson, T. (1993). *J. Med. Chem.* **36**, 3784–3794.

Macrae, C. F., Bruno, I. J., Chisholm, J. A., Edgington, P. R., McCabe, P., Pidcock, E., Rodriguez-Monge, L., Taylor, R., van de Streek, J. & Wood, P. A. (2008). *J. Appl. Cryst.* **41**, 466–470.

Partap, S., Akhtar, M. J., Yar, M. S., Hassan, M. Z. & Siddiqui, A. A. (2018). *Bioorg. Chem.* **77**, 74–83.

Sheldrick, G. M. (2015*a*). *Acta Cryst.* A**71**, 3–8.

Sheldrick, G. M. (2015*b*). *Acta Cryst.* C**71**, 3–8.

Spackman, M. A. & Jayatilaka, D. (2009). *CrystEngComm*, **11**, 19–32.

Spek, A. L. (2009). *Acta Cryst.* D**65**, 148–155.

Stoe & Cie (2002). *X-AREA* and *X-RED32*. Stoe & Cie GmbH, Darmstadt, Germany.

Tao, M., Aimone, L. D., Gruner, J. A., Mathiasen, J. R., Huang, Z., Lyons, J., Raddatz, R. & Hudkins, R. L. (2012). *Bioorg. Med. Chem. Lett.* **22**, 1073–1077.

Turner, M. J., McKinnon, J. J., Wolff, S. K., Grimwood, D. J., Spackman, P. R., Jayatilaka, D. & Spackman, M. A. (2017). *Crystal Explorer17. University of Western Australia.* http://hirshfeldsurface.net.

Zhou, G., Ting, P. C., Aslanian, R., Cao, J., Kim, D. W., Kuang, R., Lee, J. F., Schwerdt, J., Wu, H., Jason Herr, R., Zych, A. J., Yang, J., Lam, S., Wainhaus, S., Black, T. A., McNicholas, P. M., Xu, Y. & Walker, S. S. (2011). *Bioorg. Med. Chem. Lett.* **21**, 2890–2893.

supporting information

Acta Cryst. (2019). E**75**, 1880-1883 [https://doi.org/10.1107/S2056989019015147]

Crystal structure, Hirshfeld surface analysis and DFT studies of 6-[(*E*)-2-(thiophen-2-yl)ethenyl]-4,5-dihydropyridazin-3(2*H*)-one

Said Daoui, Emine Berrin Çınar, Fouad El Kalai, Rafik Saddik, Necmi Dege, Khalid Karrouchi and Noureddine Benchat

Computing details

Data collection: *X-AREA* (Stoe & Cie, 2002); cell refinement: *X-AREA* (Stoe & Cie, 2002); data reduction: *X-RED32* (Stoe & Cie, 2002); program(s) used to solve structure: SHELXT2015 (Sheldrick, 2015a); program(s) used to refine structure: *SHELXL2015* (Sheldrick, 2015b); molecular graphics: *PLATON* (Spek, 2009) and *Mercury* (Macrae *et al.*, 2008); software used to prepare material for publication: *WinGX* (Farrugia, 2012) and *PLATON* (Spek, 2009).

6-[(*E*)-2-(Thiophen-2-yl)ethenyl]-4,5-dihydropyridazin-3(2*H*)-one

Crystal data

$C_{10}H_{10}N_2OS$
$M_r = 206.26$
Monoclinic, $P2_1/c$
$a = 6.9932$ (5) Å
$b = 16.2916$ (9) Å
$c = 9.3544$ (7) Å
$\beta = 110.168$ (6)°
$V = 1000.40$ (12) Å^3
$Z = 4$
$F(000) = 432$
$D_x = 1.369$ Mg m^{-3}
Mo $K\alpha$ radiation, $\lambda = 0.71073$ Å
Cell parameters from 6992 reflections
$\theta = 2.3$–30.0°
$\mu = 0.29$ mm^{-1}
$T = 296$ K
Stick, orange
0.78 × 0.43 × 0.25 mm

Data collection

Stoe IPDS 2 diffractometer
Radiation source: sealed X-ray tube, 12 x 0.4 mm long-fine focus
Plane graphite monochromator
Detector resolution: 6.67 pixels mm^{-1}
rotation method scans
Absorption correction: integration (X-RED32; Stoe & Cie, 2002)
$T_{min} = 0.767$, $T_{max} = 0.932$
6292 measured reflections
1971 independent reflections
1394 reflections with $I > 2\sigma(I)$
$R_{int} = 0.043$
$\theta_{max} = 26.0°$, $\theta_{min} = 2.5°$
$h = -8 \rightarrow 8$
$k = -20 \rightarrow 19$
$l = -11 \rightarrow 11$

Refinement

Refinement on F^2
Least-squares matrix: full
$R[F^2 > 2\sigma(F^2)] = 0.045$
$wR(F^2) = 0.135$
$S = 1.02$
1971 reflections
131 parameters
19 restraints
Hydrogen site location: mixed
H atoms treated by a mixture of independent and constrained refinement
$w = 1/[\sigma^2(F_o^2) + (0.079P)^2]$ where $P = (F_o^2 + 2F_c^2)/3$
$(\Delta/\sigma)_{max} < 0.001$
$\Delta\rho_{max} = 0.24$ e Å^{-3}
$\Delta\rho_{min} = -0.34$ e Å^{-3}

Special details

Geometry. All esds (except the esd in the dihedral angle between two l.s. planes) are estimated using the full covariance matrix. The cell esds are taken into account individually in the estimation of esds in distances, angles and torsion angles; correlations between esds in cell parameters are only used when they are defined by crystal symmetry. An approximate (isotropic) treatment of cell esds is used for estimating esds involving l.s. planes.

Fractional atomic coordinates and isotropic or equivalent isotropic displacement parameters (Å²)

	x	*y*	*z*	U_{iso}*/U_{eq}
S1	0.23031 (12)	0.42526 (4)	0.98925 (7)	0.0768 (3)
O1	0.8844 (3)	0.41724 (11)	0.36257 (19)	0.0752 (5)
N2	0.6910 (3)	0.45665 (12)	0.66000 (19)	0.0559 (5)
N1	0.8097 (3)	0.45451 (13)	0.5682 (2)	0.0581 (5)
C4	0.5618 (3)	0.39839 (14)	0.6440 (2)	0.0521 (5)
C7	0.1949 (3)	0.34895 (13)	0.8563 (2)	0.0517 (5)
C6	0.3065 (3)	0.34666 (13)	0.7517 (2)	0.0535 (5)
H6	0.277544	0.303662	0.682065	0.064*
C5	0.4468 (3)	0.40054 (14)	0.7461 (2)	0.0549 (5)
H5	0.473561	0.443933	0.814790	0.066*
C8	0.0484 (4)	0.29384 (15)	0.8660 (2)	0.0607 (6)
H8	0.005051	0.248100	0.803758	0.073*
C1	0.7734 (3)	0.41133 (14)	0.4389 (2)	0.0568 (6)
C2	0.5880 (4)	0.35925 (15)	0.3960 (2)	0.0640 (6)
H2A	0.607918	0.311934	0.339710	0.077*
H2B	0.473610	0.390273	0.329261	0.077*
C3	0.5376 (4)	0.33001 (16)	0.5325 (3)	0.0681 (6)
H3A	0.398564	0.309944	0.499271	0.082*
H3B	0.627316	0.285060	0.581438	0.082*
C10	0.0570 (4)	0.38383 (19)	1.0572 (3)	0.0739 (7)
H10	0.023862	0.405884	1.137400	0.089*
C9	−0.0260 (4)	0.31634 (18)	0.9828 (3)	0.0713 (6)
H9	−0.124891	0.286306	1.005625	0.086*
H1	0.902 (4)	0.4897 (15)	0.593 (2)	0.058 (7)*

Atomic displacement parameters (Å²)

	U^{11}	U^{22}	U^{33}	U^{12}	U^{13}	U^{23}
S1	0.0979 (5)	0.0736 (5)	0.0729 (4)	−0.0147 (4)	0.0476 (4)	−0.0139 (3)
O1	0.0895 (12)	0.0816 (12)	0.0746 (10)	−0.0144 (10)	0.0540 (9)	−0.0103 (8)
N2	0.0594 (11)	0.0619 (11)	0.0527 (9)	−0.0040 (9)	0.0272 (8)	−0.0029 (8)
N1	0.0604 (11)	0.0644 (12)	0.0580 (10)	−0.0108 (10)	0.0312 (9)	−0.0065 (9)
C4	0.0534 (11)	0.0535 (12)	0.0522 (11)	0.0012 (10)	0.0216 (9)	−0.0007 (9)
C7	0.0521 (11)	0.0561 (13)	0.0465 (10)	0.0032 (10)	0.0165 (9)	0.0054 (9)
C6	0.0573 (12)	0.0530 (13)	0.0542 (11)	0.0002 (10)	0.0242 (10)	−0.0016 (9)
C5	0.0610 (12)	0.0565 (13)	0.0525 (11)	−0.0034 (11)	0.0261 (9)	−0.0043 (9)
C8	0.0651 (13)	0.0659 (14)	0.0543 (11)	−0.0087 (11)	0.0249 (9)	0.0049 (9)
C1	0.0655 (13)	0.0554 (13)	0.0550 (11)	0.0023 (11)	0.0279 (10)	0.0014 (9)
C2	0.0696 (14)	0.0668 (15)	0.0599 (12)	−0.0052 (12)	0.0281 (11)	−0.0118 (10)

C3	0.0757 (15)	0.0639 (15)	0.0798 (15)	−0.0133 (12)	0.0459 (13)	−0.0150 (12)
C10	0.0869 (17)	0.0885 (19)	0.0583 (13)	0.0085 (16)	0.0403 (12)	0.0062 (13)
C9	0.0686 (14)	0.0910 (18)	0.0624 (12)	−0.0097 (13)	0.0329 (10)	0.0097 (12)

Geometric parameters (Å, º)

S1—C10	1.691 (3)	C5—H5	0.9300
S1—C7	1.715 (2)	C8—C9	1.411 (3)
O1—C1	1.227 (3)	C8—H8	0.9300
N2—C4	1.283 (3)	C1—C2	1.484 (3)
N2—N1	1.385 (2)	C2—C3	1.515 (3)
N1—C1	1.345 (3)	C2—H2A	0.9700
N1—H1	0.83 (2)	C2—H2B	0.9700
C4—C5	1.446 (3)	C3—H3A	0.9700
C4—C3	1.495 (3)	C3—H3B	0.9700
C7—C8	1.388 (3)	C10—C9	1.323 (4)
C7—C6	1.448 (3)	C10—H10	0.9300
C6—C5	1.331 (3)	C9—H9	0.9300
C6—H6	0.9300		
C10—S1—C7	92.31 (13)	O1—C1—C2	123.8 (2)
C4—N2—N1	117.21 (18)	N1—C1—C2	114.77 (19)
C1—N1—N2	127.1 (2)	C1—C2—C3	112.76 (18)
C1—N1—H1	119.6 (16)	C1—C2—H2A	109.0
N2—N1—H1	112.7 (16)	C3—C2—H2A	109.0
N2—C4—C5	115.76 (19)	C1—C2—H2B	109.0
N2—C4—C3	122.57 (19)	C3—C2—H2B	109.0
C5—C4—C3	121.6 (2)	H2A—C2—H2B	107.8
C8—C7—C6	127.6 (2)	C4—C3—C2	110.5 (2)
C8—C7—S1	110.28 (16)	C4—C3—H3A	109.5
C6—C7—S1	122.15 (16)	C2—C3—H3A	109.5
C5—C6—C7	125.9 (2)	C4—C3—H3B	109.5
C5—C6—H6	117.1	C2—C3—H3B	109.5
C7—C6—H6	117.1	H3A—C3—H3B	108.1
C6—C5—C4	126.5 (2)	C9—C10—S1	112.02 (19)
C6—C5—H5	116.7	C9—C10—H10	124.0
C4—C5—H5	116.7	S1—C10—H10	124.0
C7—C8—C9	111.1 (2)	C10—C9—C8	114.3 (2)
C7—C8—H8	124.4	C10—C9—H9	122.9
C9—C8—H8	124.4	C8—C9—H9	122.9
O1—C1—N1	121.4 (2)		
C4—N2—N1—C1	18.1 (3)	S1—C7—C8—C9	−0.6 (2)
N1—N2—C4—C5	177.40 (18)	N2—N1—C1—O1	176.4 (2)
N1—N2—C4—C3	0.3 (3)	N2—N1—C1—C2	−1.9 (3)
C10—S1—C7—C8	0.74 (18)	O1—C1—C2—C3	152.4 (2)
C10—S1—C7—C6	−179.65 (18)	N1—C1—C2—C3	−29.5 (3)
C8—C7—C6—C5	−179.7 (2)	N2—C4—C3—C2	−30.2 (3)

S1—C7—C6—C5	0.8 (3)	C5—C4—C3—C2	152.9 (2)
C7—C6—C5—C4	179.0 (2)	C1—C2—C3—C4	43.3 (3)
N2—C4—C5—C6	−179.4 (2)	C7—S1—C10—C9	−0.7 (2)
C3—C4—C5—C6	−2.3 (4)	S1—C10—C9—C8	0.5 (3)
C6—C7—C8—C9	179.8 (2)	C7—C8—C9—C10	0.1 (3)

Hydrogen-bond geometry (Å, º)

D—H···*A*	*D*—H	H···*A*	*D*···*A*	*D*—H···*A*
N1—H1···O1^{i}	0.83 (3)	2.07 (3)	2.899 (3)	175 (2)
C10—H10···O1^{ii}	0.93	2.61	3.505 (3)	161

Symmetry codes: (i) −*x*+2, −*y*+1, −*z*+1; (ii) *x*−1, *y*, *z*+1.